

FILLING FACTOR DETERMINATIONS AND THEIR EFFECTS ON PLANETARY NEBULA STUDIES

D.C.V. Mallik

Indian Institute of Astrophysics
Bangalore, India

and

M. Peimbert

Instituto de Astronomía
Universidad Nacional Autónoma de México

Received 1988 July 1

RESUMEN

Hemos calculado el factor de llenado para treinta y cinco nebulosas planetarias galácticas, NP, cuyas distancias no se basan en argumentos estadísticos. Encontramos que aproximadamente la mitad de las NP de nuestra muestra tienen factores de llenado menores que 0.16. Entre más grande es la NP, menor es su factor de llenado. Este resultado implica que: a) la pendiente de la relación entre la masa y el radio es menor que la encontrada previamente; b) la masa sigue aumentando con el radio para objetos con $r > 0.1$ pc, en contradicción con las hipótesis adoptadas para obtener distancias estadísticas; c) las NP de Tipo I son ópticamente gruesas, y cinco de ellas, en nuestra muestra de ocho, tienen valores de r entre 0.1 y 0.6 pc; d) no hay correlación entre $M_{\text{polvo}}/M_{\text{gas}}$ y el radio de las nebulosas; e) el valor promedio de $M_{\text{polvo}}/M_{\text{gas}}$ es 5.2×10^{-3} , valor muy similar al del medio interestelar. Se discuten las escalas de distancias basadas en métodos estadísticos y se proponen dos nuevas escalas: una basada en los flujos observados y otra en densidades obtenidas a partir de líneas prohibidas.

ABSTRACT

We have computed the filling factor for a sample of thirty-five galactic PN for which there are distance estimates independent of statistical arguments. We found that about half of the PN in our sample have filling factors smaller than 0.16. We found a strong correlation between the filling factor and the size of the nebula in the sense that the larger the size the smaller the filling factor. Some implications of this result are: a) the slope of the mass *versus* radius relation is smaller than previously found, in better agreement with theoretical models; b) there is no flattening of the mass *versus* radius relation for $r > 0.1$ pc, contrary to assumptions made in deriving statistical distances; c) Type I PN are optically thick, and five objects in our sample of eight have r values between 0.1 and 0.6 pc; d) there is no correlation between the $M_{\text{dust}}/M_{\text{gas}}$ ratio and the radius of the nebula; e) the average $M_{\text{dust}}/M_{\text{gas}}$ ratio is 5.2×10^{-3} , value which is similar to that of the interstellar medium. A discussion of the statistical distance scales is given and two new ones are proposed, one based on the observed fluxes and another on the forbidden line densities.

Key words: NEBULAE-PLANETARY – STARS-EVOLUTION – STARS-STELLAR STATISTICS

I. INTRODUCTION

Almost all nebulae show structure on photographs. In addition to the clumpiness which gives them an inhomogeneous appearance, they show filaments, shells, bipolar geometry, density gradients, etc. The role that these spatial density variations play in determining basic parameters, like the gaseous mass and the ionization structure, is paramount to the study of the formation and evolution of planetary nebulae. It is the purpose of this paper to make a first approximation to the study of the spatial density variations by determining filling factors and their effect on different areas of PN research.

In their pioneering study of the electron density in nebulae, Seaton and Osterbrock (1957), noted that den-

sity fluctuations produced a disagreement between densities derived from forbidden-line ratios and those derived from $H\beta$ surface brightnesses. An extreme example quoted by them was NGC 7027. Osterbrock and Flather (1959) studied in detail the density distribution in the Orion nebula and showed that the densities derived from radio fluxes were considerably smaller than those derived from the $[O\ II]\ 3726/3729$ line intensity ratio, they suggested a model in which only a fraction $\epsilon \cong 0.03$ of the nebula was filled with high density material and the rest was empty. Since then ϵ has been called the filling factor and it is defined as

$$\epsilon = N_e^2(\text{rms})/N_e^2(\text{FL}) \quad , \quad (1)$$

where $N_e(\text{FL})$ is the density determined from forbidden line ratios and $N_e(\text{rms})$ is the root mean square density determined from a Balmer line or from the radio continuum flux. O'Dell (1962) using this definition of ϵ , while setting up a distance scale based on the method of statistical parallaxes and the known spectroscopic parallax of NGC 246, obtained an average value of 0.7 for ϵ and a mass of $0.14 M_\odot$ for the optically thin shells. Seaton (1966) estimated ϵ for individual nebulae by visual inspection of the photographs and drawings; for a sample of thirteen PN, he obtained values ranging from 0.2 to 1.0 and a mean of 0.63. Webster (1969) in her study of southern PN made estimates of ϵ from the details of surface brightness and dimensions of the nebulae given in the catalog of Westerlund and Henize (1967); once again the quoted values are rather large with most of them clustering around 0.8. Kaler (1970) tabulated the parameters for 250 galactic PN where again a visual estimate of the filling factors was made from photographs; in cases where a photograph was not available $\epsilon = 0.65$ was assumed. The same values were later used by Cahn and Kaler (1971) in deriving distances to galactic PN.

The first indications of a systematic variation of the filling factor with nebular size came from the photoelectric study by Torres-Peimbert and Peimbert (1977), TPP. They adopted the Cudworth (1974) distance scale and obtained $N_e(\text{rms})$ values from the observed $H\beta$ fluxes for the whole object. For most objects on their list $N_e(\text{FL}) > N_e(\text{rms})$ implying small values of ϵ . They estimated that the average filling factor was 0.05. This reduced the adopted calibration mass for the optically thin Cudworth scale from $0.50 M_\odot$ to $0.11 M_\odot$. From the observations by TPP and the distance scale of Seaton (1968) and Webster (1969) an average filling factor of 0.075 is obtained. Nevertheless, the existence of small values of ϵ was mostly ignored in studies of PN that followed.

Since the determination of ϵ required an estimate of the distance and since the measurements of the distances to individual nebulae were not very accurate, a proper analysis of the effects of the filling factor on PN studies could not be attempted.

In the last few years, the situation has changed considerably as good progress has been made in estimating distances to individual nebulae using different methods. Pottasch (1980) compiled a list of 28 PN with good distance estimates based on: spectroscopic parallaxes, interstellar extinction diagrams and the angular expansion-radial velocity method. For several of these nebulae $N_e(\text{FL})$ values had already been determined by various authors. From these data Pottasch obtained ϵ values and concluded that they are close to unity with a few nebulae having values as small as 0.3. For some of the very small nebulae ϵ was found to be larger than unity; as was pointed out by Pottasch (1984), this may be due to an underestimate of the angular size, since $N_e(\text{rms}) \propto \theta^{-3/2}$, or to the presence of large density gradients. Similarly Gathier (1987) compiled a list of 30 PN and found that $\langle \epsilon \rangle = 0.75$.

Most of the recent papers on PN have adopted values of ϵ ranging from 0.5 to 1.0. In what follows we will determine ϵ values independent of statistical distance scales, moreover we will re-examine the problem of the variation of ϵ with nebular size. A summary of this work was presented by Mallik and Peimbert (1988).

II. DETERMINATIONS OF ϵ

In this section, we will discuss three different sets of ϵ values: a) a new set of determinations based on PN with distance estimates independent of statistical distance scales, called scale independent ϵ values, b) a set of values based on the Cudworth distance scale (TPP) and, c) a set of values based on the Daub (1982) distance scale.

a) Scale Independent ϵ Values

We will adopt the definition of ϵ by Osterbrock and Flather (1959) presented in equation (1), which is the same as that adopted by TPP and by Pottasch (1980). Notice that this definition of the filling factor is the simplest; it provides only a first approximation to depict a complex density distribution since $N_e(\text{FL})$ corresponds to the average value of the high density regions while the low density regions have values different from zero.

The root mean square density of a spherical nebula is given by

$$N_e^2(\text{rms}) \propto \frac{I f(t)}{\theta^3 d}, \quad (2)$$

where I is the observed flux corrected for reddening of a Balmer line or the radio continuum flux, $f(t)$ is a known function that depends weakly on the electron temperature, θ is the angular radius of the object, and d its distance to the earth. The forbidden line method yields local densities independent of d , therefore the derived filling factor is inversely proportional to the distance adopted, that is

$$\epsilon = \frac{N_e^2(\text{rms})}{N_e^2(\text{FL})} \propto \frac{1}{d}, \quad (3)$$

and a larger statistical distance scale will yield smaller values of ϵ .

In Table 1 we present distances for 35 PN which are independent of any statistical distance scale and that have reasonably good $N_e(\text{FL})$ determinations. The distances are from: a) Gathier, Pottasch, and Pel 1986a, and Gathier, Pottasch, and Goss 1986b, based on the interstellar extinction method and 21-cm absorption measurements, b) Méndez *et al.* (1988), based on the atmospheric analysis of the central stars, c) Daub (1982), based on at least two independent methods, these objects were used by Daub to calibrate his distance scale, d) Masson (1986) from VLA observations of the expan-

TABLE 1
DISTANCES, SIZES, DENSITIES, FILLING FACTORS AND MASSES

Object (1)	d (kpc) (2)	Source of distance (3)	r (pc) (4)	N _e (rms) (10 ³ cm ⁻³) (5)	N _e (FL) (10 ³ cm ⁻³) (6)	Source of N _e (FL) [†] (7)	ε (8)	M _a (ε) (10 ⁻³ M _⊙) (9)
NGC 40	1.0	D82	0.09	1.29	2.8	K86	0.21	45.3
NGC 1535	2.1	M	0.09	1.67	5.3	K86	0.10	40.9
NGC 2346*	1.06	G1	0.15	0.27	0.7	PTP87a	0.15	37.5
NGC 2392	2.7	M	0.30	0.42	3.3	K86	0.016	150.8
NGC 2440*	2.19	G1	0.28	0.49	5.0	K86	0.010	116.1
NGC 2452 *	3.57	G1	0.19	0.54	4.5	K86	0.014	45.7
" "	3.0	D82	0.15	0.58	4.5	K86	0.017	27.3
NGC 2792	1.91	G1	0.055	2.7	3.0	TPP	0.81	42.8
NGC 2818*	3.2	T	0.305	0.18	0.5	PTP87a	0.130	198.8
NGC 2867	1.35	D82	0.039	4.62	8.9	K86	0.27	15.1
NGC 3132*	0.54	G1	0.082	0.57	0.6	K86	0.90	31.5
" "	0.84	D82	0.129	0.46	0.6	K86	0.59	80.4
NGC 3211	1.91	G1	0.064	1.74	5.0	TPP	0.12	16.6
NGC 3242	2.0	M	0.18	1.27	3.4	K86	0.14	293.6
NGC 3918	2.24	G1	0.064	3.81	6.6	K86	0.33	60.4
NGC 5315*	2.62	G1	0.031	17.	30.0	K86	0.32	30.2
NGC 6369	2.0	G2	0.143	2.71	6.0	AK87	0.20	371.
NGC 6537*	2.4	G2	0.057	7.43	12.6	K86	0.35	86.4
NGC 6567	1.68	G1	0.044	3.94	12.0	K86	0.11	11.9
" "	1.0	D82	0.026	5.1	12.0	K86	0.18	4.0
NGC 6572	0.68	D82	0.024	10.6	13.	K86	0.665	12.7
NGC 6578	2.0	G2	0.040	5.23	6.4	K85	0.67	29.0
NGC 6803	3.0	G2	0.039	6.72	10.0	K86	0.45	28.2
NGC 6804	1.35	D82	0.203	0.28	0.7	K86	0.16	99.1
NGC 6884	1.8	G2	0.028	9.73	10.0	TPP	0.95	22.1
NGC 6886	1.7	G2	0.024	7.52	10.0	K86	0.565	8.3
NGC 6891	3.8	M	0.136	2.7	5.0	AK87	0.29	357.0
NGC 7009	2.4	M	0.150	2.07	6.0	PTP87b	0.119	254.8
NGC 7026	2.5	G2	0.155	1.17	8.0	K86	0.021	66.2
" "	1.78	D82	0.11	1.38	8.0	K86	0.030	33.8
NGC 7027	0.94	MA	0.038	17.2	80.0	PTP87b	0.046	21.4
NGC 7293*	0.30	M	0.56	0.043	0.162	H78	0.07	210.6
NGC 7354	1.5	G2	0.114	1.55	4.0	AK87	0.15	94.0
IC 418	2.0	M	0.059	9.60	15.0	PTP87b	0.41	133.6
IC 1747	2.5	G2	0.077	2.15	3.0	K86	0.51	73.9
" "	2.25	D82	0.069	2.26	3.0	K86	0.57	59.5
IC 2448	3.5	M	0.075	2.28	12.0	K86	0.036	19.3
He 2-108	8.3	M	0.22	0.77	2.0	K86	0.148	333.3
He 2-131	0.59	G1	0.008	22.5	20.0	K86	1.26	1.2
He 2-138	5.0	M	0.086	2.96	8.0	TPP	0.137	73.7

† AK 87: Aller and Keyes 1987; D82: Daub 1982; G1: Gathier *et al.* 1986a; G2: Gathier *et al.* 1986b; H78: Hawley 1978; K85: Kaler 1985; K86: Kaler 1986; M: Méndez *et al.* 1988; MA: Masson 1986; PTP 87a: Peimbert and Torres-Peimbert 1987a; PTP 87b: Peimbert and Torres-Peimbert 1987b; T: Tifft *et al.* 1972; TPP: Torres-Peimbert and Peimbert 1977.

* Type I PN.

sion of NGC 7027 and, e) Tifft, Connolly, and Webb (1972), by assuming that NGC 2818 belongs to the cluster with the same name. The samples of Gathier *et al.* and Méndez *et al.* in Table 1 are mutually exclusive. The N_e(rms) values given in Table 1 have been determined from the equation

$$N_e \text{ (rms)} = 1.57 \times 10^5 \left[\frac{S}{\theta^3 d} \right]^{1/2} \quad , \quad (4)$$

where S is the 5 GHz flux in 10⁻²³ erg cm⁻² s⁻¹ Hz⁻¹, θ, the angular radius given in arcseconds, and d, the distance in kiloparsecs. The radio fluxes and the angular radii

have been taken from the compilation by Daub (1982). The forbidden line densities are based mainly on measurements of the [O II] and [S II] line ratios and in some cases of the [Cl III] and [Ar IV] line ratios; they have been mostly taken from Kaler (1986) supplemented by data from Peimbert and Torres-Peimbert (1987a, 1987b) and Aller and Keyes (1987). The sources of the $N_e(\text{FL})$ value and the ϵ value are presented in columns (7) and (8) of Table 1, respectively.

For NGC 7293, the measurements by Hawley (1978) were added to obtain integrated [S II] fluxes representative of the entire nebula and from these, the $N_e(\text{FL})$ was derived.

The filling factors have been plotted against the radii for all the objects in Figure 1. When a nebula has more than one independent value of the distance in Table 1, its positions on Figure 1 have been connected by a dashed line. Before discussing this figure, we must discuss the observational selection effects on the sample.

We have two possible selection effects; a) how representative of galactic PN is the sample of known PN (for example those in the Perek Kohoutek catalogue), and b) how representative of the known galactic PN is the sample in Table 1.

To the first question we have two observations to make: (i) large nebulae have low surface brightness and all observational methods preferentially select against them; excepting NGC 7293 this would explain the absence of very large nebulae in our sample, (ii) due to interstellar reddening the incompleteness of the sample of known PN is larger for objects towards the galactic center; in this sense known PN are more representative of the solar neighborhood.

To answer the second question, we need to know if there was a selection effect in the three parameters needed to place an object in Table 1, namely: flux, distance and $N_e(\text{FL})$.

We consider that there is no selection effect due to the flux since most known PN with distances smaller than about 3 kpc have measured radio and Balmer lines fluxes.

Distances based on interstellar extinction and 21-cm absorption require the nebula to be in, or close to, the galactic plane and at large enough distances to show significant reddening and 21-cm absorption; since PN show a strong concentration to the plane there is no obvious observational selection involved here. The sample by Méndez *et al.* (1988) does not utilize any property of the nebula and is based on properties of the central star; the method depends upon the presence of absorption lines in the stellar spectra of bright O type stars. Moreover, a strong nebular continuum contaminates the stellar spectrum, therefore the sample avoids smaller high surface brightness nebulae. In a sense, the sample of Méndez *et al.* is complementary to those of Gathier *et al.* (1986a,b). This produces a more representative distribution of sizes.

The major selection effect is produced by $N_e(\text{FL})$, since forbidden line ratios are almost insensitive below $300 - 400 \text{ cm}^{-3}$. Hence filling factors are difficult to determine for large PN. We have considered this effect in some detail and determined the region of the ϵ versus r diagram that is inaccessible to ϵ determinations. For nebulae that are ionization bounded, we have used the optically thick distance scale by Cudworth (1974) given by

$$d = 0.0178 I(\text{H}\beta)^{-1/2} \text{ pc}, \quad (5)$$

which corresponds to

$$r = 14.73 \epsilon^{-1/3} N_e^{-2/3} \text{ pc}. \quad (6)$$

In Figure 1 we have drawn two lines for $N_e(\text{FL})$ equal to 500 and 1000 cm^{-3} ; in general it is not possible to place objects to the right of these lines in this diagram. It is possible to find a similar restriction for optically thin nebulae (density bounded) by assuming that they have a mass given by

$$M(\epsilon) = \epsilon^{1/2} M(\text{rms}) \quad (7)$$

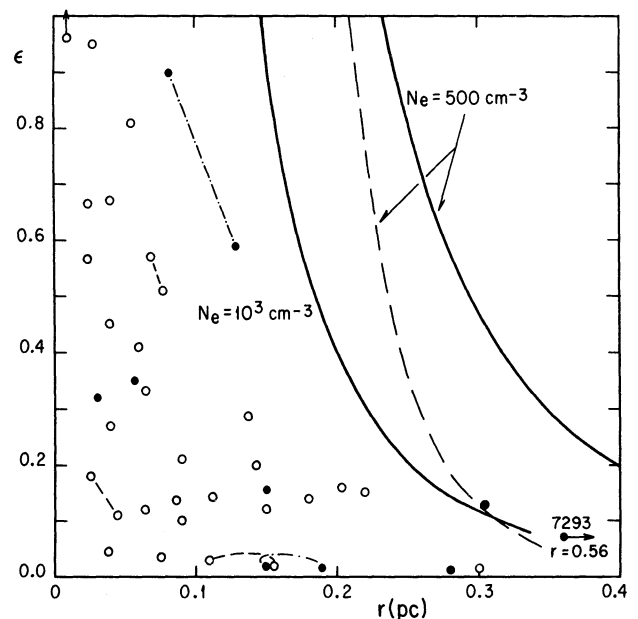


Fig. 1. Filling factor versus radius diagram for PN with scale-independent distances. Filled circles denote Type I PN, open circles the rest. Those circles joined by broken lines denote the same object with two different distance estimates as given in Table 1. The areas to the right of the solid lines correspond to optically thick PN with $N_e(\text{FL})$ smaller than 10^3 and 500 cm^{-3} respectively, while the area to the right of the broken line corresponds to optically thin PN with $N_e(\text{FL})$ smaller than 500 cm^{-3} (see text).

with $M(\text{rms}) = 0.50 M_{\odot}$ (Cudworth 1974), therefore

$$r = 1.677 \epsilon^{-1/6} N_e^{-1/3} \text{ pc.} \quad (8)$$

From the previous discussion, we consider that the sample in Table 1 is representative of the known PN in the solar vicinity with r values smaller than 0.2 pc, we consider that there are no strong observational effects against objects inside the permitted region in Figure 1. Observational selection prevents nebulae with low density and large filling factors from being discovered. However, even if we presume that this effect is pronounced at densities as high as 500 cm^{-3} , we still have a huge gap in our permitted region where there are almost no PN with large r and large ϵ . For $r > 0.14$ pc the twelve objects have $\epsilon < 0.21$ while for $r > 0.08$ only two out of eighteen have $\epsilon > 0.22$. We therefore conclude that a real effect of decreasing filling factors with increasing size independent of the effects of observational selection is present.

From the sample in Figure 1 we obtain

$$\log \epsilon = -(1.74 \pm 0.21) - (0.91 \pm 0.18) \log r, \quad (9)$$

with a correlation coefficient of -0.65 . From the data in Table 1 and equation (9) we obtain that the average difference between the "observed" ϵ and the predicted ϵ is a factor of 2.14, i.e. that the mean $|\log(\epsilon_i/\epsilon_{\text{pred}})|$ is 0.33.

b) Daub's ϵ Values

A much larger sample of nebulae is available for similar analysis if one uses the statistical distance scales. In Figure 2 we present the ϵ versus r diagram for Daub's (1982) sample and his distance scale. From arguments given above, we also show in Figure 2 the region inaccessible to filling factor determinations; the boundaries have been drawn for two densities on the assumption that the objects are optically thin and have a mass given by equation (7) with $M(\text{rms}) = 0.14 M_{\odot}$. The $M(\text{rms})$ value was chosen to be consistent with the Daub distance scale. The $N_e(\text{FL})$ sources were the same as for PN in the distance independent sample.

It is remarkable that very few large nebulae with moderate to high filling factors ($\epsilon > 0.2$) are present in Figure 2. An increase in the distance scale will lower the ϵ values and will not destroy the trend present in Figure 2. From this sample it also follows that ϵ decreases with size.

For objects with $r > 0.12$, $\langle \epsilon \rangle$ is 0.10 for Type I PN and 0.08 for the rest of the sample, i.e., there is no significant difference in the $\langle \epsilon \rangle$ value between both sub-samples.

From the Daub sample we obtain

$$\log \epsilon = -(1.74 \pm 0.22) - (0.92 \pm 0.20) \log r, \quad (10)$$

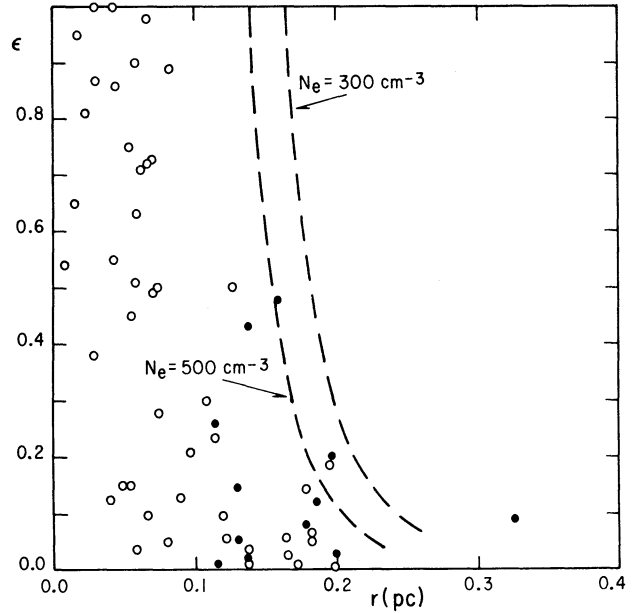


Fig. 2. Same as Figure 1 but for PN in Daub's (1982) sample adopting the Daub distance scale. The area to the right of the broken lines corresponds to optically thin PN with $N_e(\text{FL})$ smaller than 500 and 300 cm^{-3} respectively.

with a correlation coefficient of -0.61 and in excellent agreement with the relation found for the scale independent sample.

c) Cudworth's ϵ Values

In Figure 3 we present the ϵ versus r diagram for nebulae in the TPP sample based on the Cudworth (1974) distance scales for optically thick and optically thin objects. As in Figure 1 we show the region inaccessible to ϵ determinations for optically thin objects based on equation (7) for $M(\text{rms}) = 0.50 M_{\odot}$.

Figure 3 also shows the correlation between ϵ and r , in the sense that the higher the r value the smaller the ϵ value. From this sample we obtain

$$\log \epsilon = -(2.38 \pm 0.28) - (1.38 \pm 0.25) \log r, \quad (11)$$

with a correlation coefficient of -0.74 .

d) Variations of ϵ with Radius

Any changes in the distance estimates will move the nebulae in Figures 1-3 but will preserve the appearance of the diagrams. Moreover, a change in the distance scale will preserve the slope of the $\log \epsilon$ versus $\log r$ relation. The conclusion seems inescapable: the filling factor of the three observed samples of PN shows a rather remarkable correlation with size in the sense that larger nebulae have smaller filling factors.

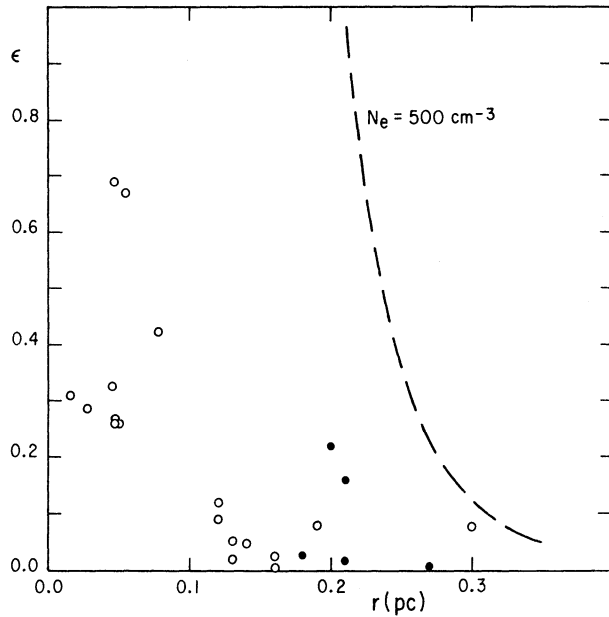


Fig. 3. Same as Figure 1 but for PN in TPP's sample adopting the Cudworth (1974) distance scales for optically thick and optically thin PN. The area to the right of the broken line corresponds to optically thin PN with $N_e(\text{FL}) < 500 \text{ cm}^{-3}$.

We will advance the hypothesis that the variation of ϵ with r is due to mass loss from the central star. It has been argued that the shaping of PN is due to the interaction of material ejected from the central stars at different velocities, the so called two or several wind models (e.g., Peimbert 1985 and references therein). We propose that the main cause for the decrease of ϵ with r is the mass-loss episode at velocities of several thousand km s^{-1} , when the star is hot enough to start to ionize the nebula, that occurs after a previous mass-loss episode at velocities of about 20 km s^{-1} , when the star is in the asymptotic giant branch. The high velocity mass-loss process is responsible for: a) the central cavity, which increases with time, b) the production of clumps and filaments by the Rayleigh-Taylor instability (Cappiotti 1973; Kahn 1983); this production should also increase with time since the momentum ratio of the high velocity material to the low velocity material also increases with time. The presence of spatial density fluctuations produces two additional effects that decrease the value of ϵ : PN could be optically thicker in some directions than in others therefore the adopted radius might be larger than the average one, moreover $M(\epsilon)$ will be the mass of the ionized material without including the mass of the neutral material within the adopted radius.

Density fluctuations are particularly pronounced in Type I PN; these objects show bipolar structures consisting of low density material with filaments, lobes, and ansae along the major axis and of higher density

material along the minor axis (see Peimbert 1985 for a discussion on the formation of Type I PN).

III. MASS VERSUS RADIUS RELATION

The ionized mass of a spherical PN of volume V , density $N_e(\text{FL})$ and filling factor ϵ is given by

$$\begin{aligned} M(\epsilon) &= \langle m \rangle \epsilon N_e(\text{FL}) V, \\ &= \langle m \rangle \epsilon^{1/2} N_e(\text{rms}) V, \\ &= \epsilon^{1/2} M(\text{rms}), \end{aligned} \quad (12)$$

where $\langle m \rangle$ is the mean atomic mass per free electron. For $N(\text{He})/N(\text{H}) = 0.1$, $N(\text{H}^+) = 0.8 N_e$, expressing the radius in parsecs and the mass in M_\odot equation (12) can be written as

$$M(\epsilon) = 0.106 \epsilon N_e(\text{FL}) r^3. \quad (13)$$

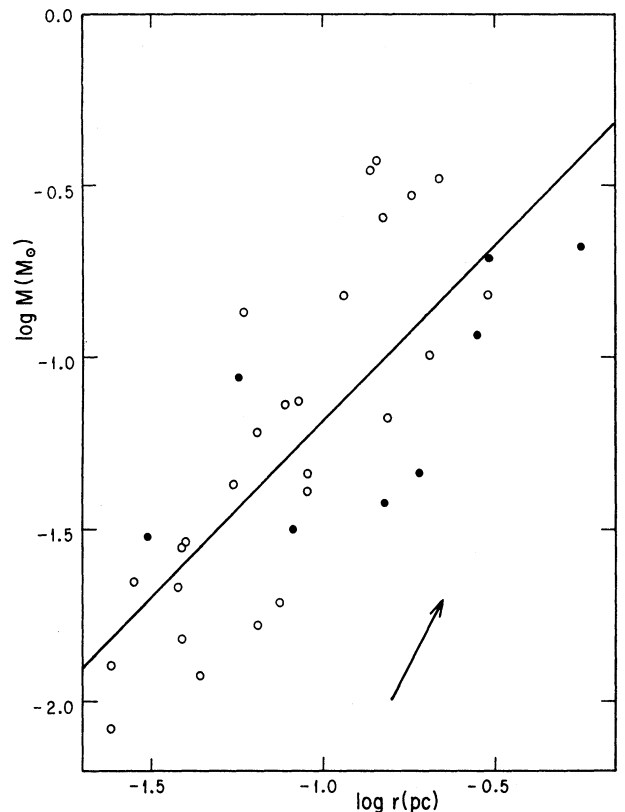


Fig. 4. Mass versus radius diagram for PN with scale-independent distances. Filled circles Type I PN, open circles the rest. The straight line is the least squares fitting to the data given by $\log M(\epsilon) = (-0.16 \pm 0.17) + (1.02 \pm 0.15) \log r$; with a correlation coefficient of 0.77. The arrow indicates the change in mass if an object is 1.4 times farther away than assumed.

TABLE 2
MASS VERSUS RADIUS RELATION^a

Radii range (pc)	ϵ values	α M (ϵ)	α M (rms)	Correlation Coefficient	Sample ^b
0.01 – 0.56	0.01 – 1.0	1.02 ± 0.15	...	0.77	1
0.01 – 0.33	1.0	...	1.43 ± 0.09	0.95	2
0.004 – 0.96	1.0	...	2.46	0.86	3a
0.032 – 0.27	1.0	...	1.88	0.77	3b
0.007 – 0.066	1.0	...	1.47 ± 0.12	0.92	4
0.004 – 0.12	0.01 – 1.0	1.21 ± 0.10	5a
0.12 – 0.46	...	0	5b

a. Given by $M \propto r^\alpha$. b. (1) This paper, scale independent sample; (2) Pottasch 1980; (3a) Phillips and Pottasch 1984; (3b) Phillips and Pottasch 1984, $0.002 < M(\text{rms})/M_\odot < 0.20$; (4) Gathier *et al.* 1983; (5a) Daub 1982, optically thick sample; (5b) Daub 1982, optically thin sample under the assumption of a constant mass.

In column 9 of Table 1 we present the $M(\epsilon)$ values for the scale independent sample. Figure 4 shows a plot of $M(\epsilon)$ versus r on a logarithmic scale. The mass increases with r and does not show any effect of saturation at large r values. Our result agrees with those by Pottasch (1980), Phillips and Pottasch (1984), and Gathier (1987) in the sense that most objects are optically thick in at least some directions.

From a least squares fit to the data in Table 1, we find

$$\log M(\epsilon) = -(0.16 \pm 0.17) + (1.02 \pm 0.15) \log r, \quad (14)$$

with a correlation coefficient of 0.77, and where He 2–131 was not included; equation (14) is also plotted in Figure 4. This result is presented in Table 2 together with similar determinations by other authors.

Several authors have determined ionized masses of PN in recent years and have obtained relations between masses and radii that are steeper than ours (see Table 2). In most of these determinations ϵ has been assumed to be unity and its variation with radius has been ignored. Pottasch (1980) and Gathier *et al.* (1983) used $M(\text{rms})$ values instead of $M(\epsilon)$ values; if in their samples $\epsilon \propto r^{-0.91}$ then from equation (12) it would follow that: $M(\epsilon) \propto r^{0.98}$ from the sample by Pottasch and $M(\epsilon) \propto r^{1.02}$ from the sample by Gathier *et al.* (1983), in excellent agreement with our result.

The slope derived by Phillips and Pottasch (1984) is considerably larger than ours. Notice that if their sample is reduced to objects in the 0.032 to 0.27 range, the slope becomes substantially smaller, moreover, if there is a systematic variation between ϵ and r of the type found in this paper the slope would become even smaller.

Daub (1982) attempted a filling-factor independent plot of mass versus surface brightness, the latter being a measure of the size, and found that for $r > 0.12$ pc the mass stops growing. He obtained $0.14 M_\odot$ for the op-

tically thin limit assuming $\epsilon = 1$. In Table 1 many of the objects have $M(\epsilon)$ larger than $0.14 M_\odot$, therefore not only most PN with r between 0.12 and 0.5 seem to be optically thick but their $M(\text{rms})$ value is considerably larger than $0.14 M_\odot$, and consequently the Daub distance scale is too short.

IV. DUST TO GAS RATIO

Several authors have found that the $M_{\text{dust}}/M_{\text{gas}}$ ratio decreases by two to three orders of magnitude with the size of PN (Nata and Panagia 1981; Pottasch *et al.* 1984; Pottasch 1987; Lenzuni *et al.* 1987). The dust mass was obtained from the far infrared flux of these nebulae utilizing the equation

$$M_{\text{dust}} = \frac{4 \pi a^2 \rho F_\nu}{3 Q_\nu B_\nu (T_D)} \quad (15)$$

where a is the size of the grains, ρ their intrinsic density, Q_ν the emissivity, and T_D the dust temperature; Pottasch (1984) has suggested $a/Q_\nu = 1 \times 10^{-3}$ for $\lambda = 60 \mu\text{m}$, and $\rho = 3 \text{ g cm}^{-3}$.

We have used the distances from Table 1 and the fluxes and dust temperatures given by Pottasch (1984) to derive M_{dust} of seventeen nebulae from our sample and hence estimated $M_{\text{dust}}/M(\epsilon)_{\text{gas}}$. The results are given in Table 3 and displayed in Figures 5 and 6. We do not find any correlation of this ratio with size or filling factor of the nebulae. The average value of $M_{\text{dust}}/M(\epsilon)_{\text{gas}}$ for the seventeen objects is 5.2×10^{-3} ; this value is similar to the value of 7×10^{-3} estimated by Savage and Mathis (1979) for diffuse clouds in the galaxy.

It is well known that Fe, Si, Mg and Al are depleted in gaseous envelopes of PN (e.g., Shields 1978, 1983; Pwa, Pottasch, and Mo 1986). From the abundances representative of the solar photosphere, "local galactic", tabulated by Meyer (1985) we compute a mass fraction

TABLE 3
DUST TO GAS MASS RATIOS

Object	Radius (10 ¹⁷ cm)	F25 μm (Jy)	T _D (°K)	M _d (10 ⁻⁵ M _⊙)	M _d /M _g (10 ⁻³)
NGC 40	2.7	79.2	141.	12.5	2.76
NGC 2346 ^a	4.5	0.9	50.	44.4	11.8
NGC 2392	9.0	10.4	95.	81.2	5.38
NGC 2440 ^a	8.4	29.	115.	51.6	4.44
NGC 2818 ^a	6.9	1.0	51.	110.6	5.56
NGC 2867	1.2	16.	130.	6.8	4.52
NGC 3242	5.4	38.	115.	60.4	2.1
NGC 3918	1.9	65.8	145.	44.6	7.38
NGC 6369	4.3	74.	110.	143.6	3.87
NGC 6572	0.72	177.	180.	5.1	4.0
NGC 6804	6.1	15.7	118.	10.1	1.02
NGC 6884	0.84	15.	140.	8.1	3.67
NGC 6886	0.7	12.8	130.	7.9	9.52
NGC 7009	4.5	49.	113.	164.6	6.45
NGC 7026	3.3	21.	100.	54.5	8.23
NGC 7354	3.4	41.	115.	36.9	3.93
IC 418	1.8	224.	190.	43.1	3.22

a. Type I PN.

of 2.7×10^{-3} for these elements. From the assumptions that: about 15% of the oxygen is locked in silicate cores, about $5\% \pm 5\%$ is located in polymer mantles (Meyer 1985), and that most of Fe, Si, Mg and Al are in dust grains, we would expect a total $M_{\text{dust}}/M_{\text{gas}}$ of about 4.6×10^{-3} , in excellent agreement with the average value derived from Table 3.

From equations (3), (12) and (15) it follows that $M_{\text{dust}}/M(\epsilon)_{\text{gas}}$ is independent of the distance to an object. It is unlikely that errors in the infrared fluxes, $H(\beta)$ fluxes, sizes and $N_e(\text{FL})$ are large enough to alter

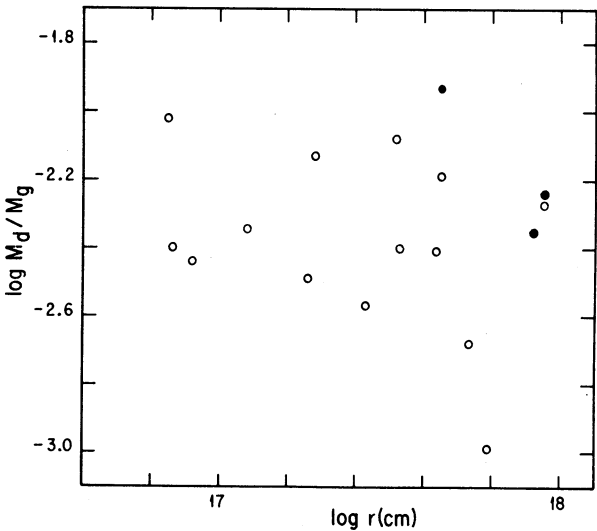


Fig. 5. Dust to gas ratio versus radius diagram for PN presented in Table 2. Filled circles Type I PN, open circles the rest.

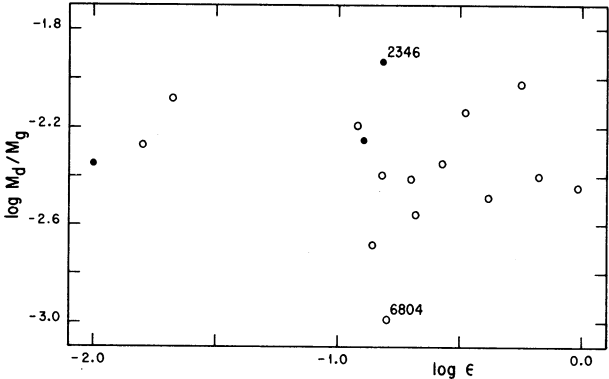


Fig. 6. Dust to gas ratio versus filling factor for the PN in Figure 5.

significantly the plot in Figure 5. We presume that the earlier result where $M_{\text{dust}}/M(\text{rms})_{\text{gas}}$ decreased appreciably with increasing r , was due in part to the effect of the filling factor decreasing with r .

V. DISTANCE SCALES

a) Scale Independent Sample

In Figure 7 we present the emitted $H\beta$ flux, $E(H\beta)$, versus radius relation for the scale independent sample. The first striking result is that there is no decrease of $E(H\beta)$ with radius which implies that the sample does not become optically thin, in agreement with §III. Secondly, for a given radius there is a scatter in $E(H\beta)$ of about an order of magnitude; we consider that the scatter is real and that it is mainly due to the different amount of Lyman continuum photons produced by the central stars.

Under the assumption that all the objects are optically thick, the average emitted flux, weighted by the logarithm, is $\langle E(H\beta) \rangle = 3.50 \times 10^{34} \text{ erg s}^{-1}$ which yields a distance scale given by

$$d = 0.0171 I(H\beta)^{-1/2}, \quad (16)$$

where d is given in pc and $I(H\beta)$ in $\text{erg cm}^{-2} \text{ s}^{-1}$. To obtain equation (16) and $\langle E(H\beta) \rangle$ we excluded He 2–131 because the central star might be in a very early stage of evolution before being close to its maximum production of Lyman continuum photons, we also excluded NGC 7293 because its central star is already in the descending branch with apparently a diminishing temperature (Méndez *et al.* 1988). A similar situation might be prevailing in NGC 2818, which was also excluded.

We conclude from the previous discussion and the discussion in §III, that most PN in the solar vicinity are optically thick at least in some directions.

There are two well known objects of the solar vicinity that are optically thin: NGC 2242 and NGC 4361 (e.g.,

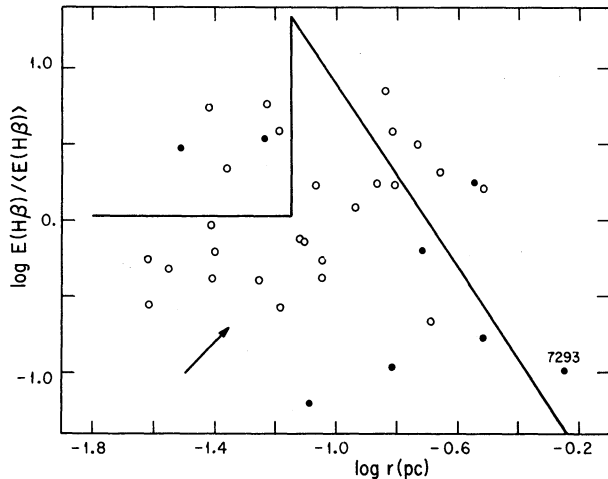


Fig. 7. Log $E(H\beta)$ versus log r diagram for the scale-independent sample. $\langle E(H\beta) \rangle = 3.50 \times 10^{34} \text{ erg s}^{-1}$. The horizontal line and the diagonal line correspond to the optically thick and optically thin distance scales respectively by Cudworth (1974). His optically thin scale crosses our optically thick scale at $r = 0.20 \text{ pc}$. The arrow indicates the displacement of any given point if its distance is increased by a factor of 1.4.

Torres-Peimbert *et al.* 1988), but by and large most well known PN in the solar vicinity are optically thick. NGC 2242 is not in Table 1 because there is no reliable distance determination for it nor NGC 4361, because there is no reliable filling factor determination for it.

We recommend equation (16) to obtain distances to PN with radius in the 0.02 to 0.30 pc range. For any given object the error in the distance could be as large as a factor of three, but in general, it will be smaller than a factor of two, which amounts to a difference of 0.6 in the log $E(H\beta)/\langle E(H\beta) \rangle$ value in Figure 7.

b) Cudworth's Distance Scales

For optically thick PN with $r < 0.07 \text{ pc}$, Cudworth (1974) obtained

$$d = 0.0178 I(H\beta)^{-1/2}, \quad (17)$$

under the assumption of the same $E(H\beta)$ for all objects; the mean value corresponds to $\langle E(H\beta) \rangle = 3.79 \times 10^{34} \text{ erg s}^{-1}$.

Alternatively from PN with $r < 0.07 \text{ pc}$ in the scale-independent sample (fourteen objects disregarding He 2-131) we obtain $\langle E(H\beta) \rangle = 3.62 \times 10^{34} \text{ erg s}^{-1}$, which corresponds to a constant of 0.0174 in equation (17) in excellent agreement with Cudworth's result. Moreover, from PN with $r \geq 0.07 \text{ pc}$ in the scale independent sample, (eighteen objects disregarding NGC 2818 and NGC 7293) we obtain $\langle E(H\beta) \rangle = 3.38 \times 10^{34} \text{ erg s}^{-1}$, which corresponds to a constant of 0.0168 in equation (17). This result is in excellent agreement with our value for objects with $r < 0.07$ and supports our hypothesis that

most PN in the scale independent sample are optically thick.

For PN with $r > 0.07$ Cudworth (1974) assumed that $M(\text{rms}) = 0.50 M_{\odot}$ and that they were optically thin. For objects with $r > 0.07$ in our sample, we obtain $M(\text{rms}) = 0.48 M_{\odot}$ in excellent agreement with the mass adopted by Cudworth.

In Figure 7 we present the implied $E(H\beta)$ fluxes from Cudworth's distance scales. The horizontal line corresponds to the optically thick distance scale while the diagonal corresponds to the optically thin distance scale. We would like to make a few comments: a) the discontinuity at $r = 0.07 \text{ pc}$ predicted by Cudworth is not present in the scale-independent sample. b) By adopting a constant mass for PN with $r > 0.07 \text{ pc}$, Cudworth is overestimating the masses and the distances for objects in the 0.07 to 0.20 pc range and he is underestimating the masses and distances for objects with $r > 0.20 \text{ pc}$. c) At least in the case of NGC 7293 we propose that $E(H\beta)$ is small because the central star is becoming fainter (Méndez *et al.* 1988) and not because the object is optically thin; moreover, the presence of molecules (Storey 1984) indicates that the object has never been optically thin in all directions. Consequently some large nebulae might fit Cudworth's optically thin distance scale not because the objects are optically thin, but because the central star is fading. The second largest nebula in the scale-independent sample is NGC 2818 which also shows molecular hydrogen emission (Storey 1984).

Moreover, it should also be mentioned that many PN of Type I are larger than 0.07 pc and that all of them are optically thick, contrary to the hypothesis by Cudworth. For example the five Type I PN in the TPP sample have r values larger than 0.17 pc and are optically thick.

c) Daub's Distance Scale

In Daub's sample all Type I PN, twelve objects in all, have r values larger than 0.1 pc, and ten of these have values larger than 0.12 pc (see Figure 2). Moreover, Type I PN are optically thick, in at least some directions, as is shown by their strong [O I] and [N I] lines as well as by the presence of molecular lines (e.g., Huggins and Healy 1986a, 1986b; Zuckerman and Gatley 1988; Rodríguez 1988 and references therein). Consequently one of the hypotheses on which the Daub distance scale is based, namely that all the objects with $r > 0.12 \text{ pc}$ are optically thin, is not valid. Another argument against this distance scale follows from the increase of nebular mass with radius in the scale-independent sample (see §III).

The $\langle M(\text{rms}) \rangle$ value for PN with $r > 0.12$ in the scale-independent sample (comprising 13 objects) is $0.67 M_{\odot}$ which is considerably larger than the $M(\text{rms}) = 0.14 M_{\odot}$ value adopted by Daub. Consequently the Daub distance scale is shorter than both ours and the Cudworth distance scale.

d) $N_e(\text{FL})$ Distance Scale

In Figure 8 we present the $N_e(\text{FL})$ versus radius diagram as well as a least squares fit to the data given by

$$\log N_e(\text{FL}) = (2.66 \pm 0.20) - (0.96 \pm 0.17) \log r, \quad (18)$$

with a correlation coefficient of -0.70 and where r is given in pc. This equation should provide good distance estimates for objects with $r < 0.20$ pc. For larger objects the diagnostic ratios become almost density independent. We consider that in the future a $N_e(\text{FL})$ versus r relation might prove to yield a better distance scale than that given by equation (16). To improve this relation we need higher accuracy in the [Cl III] atomic parameters as well as more and better observational data for the [S II], [O II], [Cl III] and [Ar IV] density determinations.

Sabbadin *et al.* (1984) obtained a similar relation between $N_e(\text{rms})$ and r for PN with $r < 0.1$ pc, i.e. $N_e(\text{rms}) \propto r^{-1}$. For PN with $r > 0.1$ pc they found a change of slope given by $N_e(\text{rms}) \propto r^{-3}$ and concluded that the larger nebulae in their sample are optically thin. Our scale shows no sign of this change in slope. Phillips and Pottasch (1984) obtained a steeper relation given by $N_e(\text{rms}) \propto r^{-1.34}$. From equations (1), (9) and (18) we obtain $N_e(\text{rms}) \propto r^{-1.42}$ for the scale independent sample, a relation which is quite similar to that by Phillips and Pottasch.

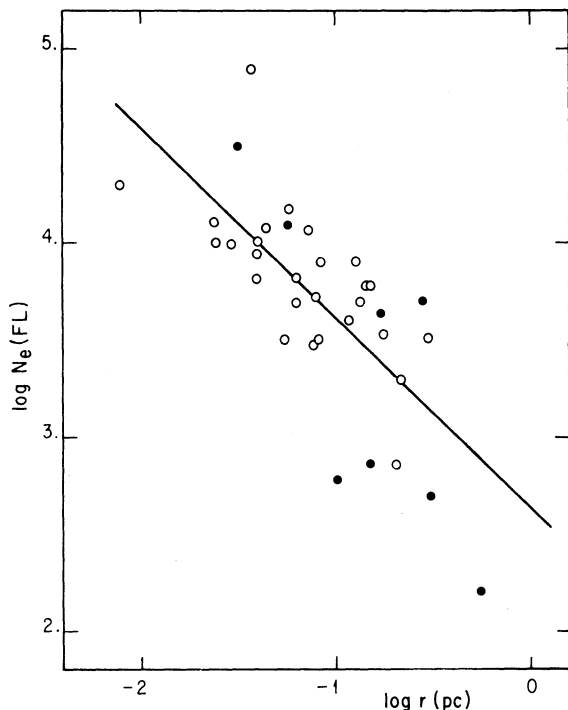


Fig. 8. $N_e(\text{FL})$ versus r diagram for the scale-independent sample. The straight line is the least squares fit to the data given by $\log N_e(\text{FL}) = (2.66 \pm 0.19) - (0.96 \pm 0.17) \log r$; with a correlation coefficient of -0.70 .

VI. CONCLUSIONS

From a distance scale independent sample of 35 PN we found values of ϵ in the 0.01 to 1 range with about half of the objects having ϵ smaller than 0.16. By comparing the continuum emission derived from the optically thin and optically thick parts of the spectrum Terzian and Dickey (1973) concluded that most of the radiation in their PN sample originates in clumps, in good agreement with the low values of ϵ presented in this paper.

We found that for the scale independent sample: *i*) the filling factor decreases with size as $\epsilon = 0.0182 (r/\text{pc})^{-0.91}$, *ii*) the mass increases with size as $M(\epsilon) = 0.692 (r/\text{pc})^{1.02} M_\odot$ and consequently $M(\text{rms}) \propto r^{1.48}$. The increase of $M(\epsilon)$ with size implies that the large majority of the PN in our sample are optically thick.

The $M_{\text{dust}}/M(\epsilon)$ ratio for the scale independent sample is uncorrelated with size. It is also uncorrelated with ϵ . Our result is in disagreement with previous investigations and apparently implies that there is no substantial dust destruction with time in the nebular shells. The average $M_{\text{dust}}/M(\epsilon)$ value for 17 PN is 5.2×10^{-3} , a value that is distance independent, and that is similar to that found in the interstellar medium.

The decrease of the $M_{\text{dust}}/M(\text{rms})$ ratio with r found by other authors in other samples might be due in part to an ϵ variation with size and in part to the presence, in other samples, of population II PN with lower heavy element abundances and smaller shell masses which would artificially increase their distances in relation to those of population I PN.

A statistical distance scale given by $\langle E(\text{H}\beta) \rangle = 3.5 \times 10^{34} \text{ erg s}^{-1}$ follows from the scale-independent sample for objects in the $0.01 < r < 0.3$ pc range. The PN formation rate derived from this distance scale is almost the same as that derived from the Cudworth (1974) distance scale and is in good agreement with the white dwarf formation rate, but it is lower than the formation rates derived from Miras or OH/IR stars (e.g., Phillips 1988). Our statistical distance scale is also in good agreement with that derived from the galactic rotation curve by Schneider and Terzian (1983).

Also note that if the total number of ionizing photons is constant during the evolution of PN, then $N_e^2(\text{rms}) r^3 = \text{const.}$, or $\epsilon N_e^2(\text{FL}) r^3 = \text{const.}$; since the mass is given by $M(\epsilon) \propto \epsilon N_e(\text{FL}) r^3$ it follows that $M(\epsilon) \propto \epsilon^{1/2} r^{3/2}$, furthermore and since according to equation (9) the scale-independent sample yields $\epsilon \propto r^{-0.91}$, it follows that $M(\epsilon) \propto r^{1.04}$ in excellent agreement with relation (14). Therefore the assumption that the number of ionizing photons is constant during PN evolution is consistent with the properties of the scale-independent sample and with the distance scale proposed by us.

For objects smaller than 0.07 pc our distance scale agrees with the optically thick distance scale by Cudworth (1974). The $M(\text{rms})$ value for PN with r larger than 0.07 is $0.48 M_\odot$, in very good agreement with the

value of $0.50 M_{\odot}$ derived by Cudworth. For objects in the $0.07 < r < 0.20$ pc range, the Cudworth optically thin scale systematically overestimates the distances, while for larger objects it underestimates them, with the exception of optically thick PN with fading central stars like NGC 7293.

The $\langle M(\text{rms}) \rangle$ value for PN larger than 0.12 pc is $0.67 M_{\odot}$ for the scale-independent sample, a value considerably larger than $0.14 M_{\odot}$, the adopted value by Daub (1982). Consequently, the Daub distance scale is shorter than ours by a factor of 1.87 for objects in the $0.12 < r < 0.3$ pc range.

Out of the 12 Type I PN in Daub's (1982) sample, 10 have radii larger than 0.12. They are known to be optically thick from other evidences, contrary to Daub's assumption that all PN with $r > 0.12$ pc are optically thin. A similar situation with respect to PN of Type I prevails in Cudworth's (1974) sample.

We found a relation between $N_e(\text{FL})$ and size given by:

$$r(\text{pc}) = 589 (N_e)^{-1.04},$$

which can be used as a distance scale for objects in the 0.01 to 0.2 pc range.

It is a pleasure to thank R.H. Méndez for sending us the results of their atmospheric analysis of central stars and distance determinations in advance of publication. We would also like to thank M. Peña, A.V. Tutukov, S. Torres-Peimbert, L.F. Rodríguez, G. Stasinska and R. Costero for fruitful discussions. We thank J.F. Barral for assistance with some of the computations. This paper was written while one of us (D.C.V.M.) was on a three-month long visit to the Instituto de Astronomía, UNAM. He acknowledges with gratitude the generous support of UNAM and CONACYT which made the visit possible and remembers with pleasure the stimulating environment provided by the colleagues at the Instituto de Astronomía which made it such an enjoyable experience.

REFERENCES

- Aller, L.H. and Keyes, C.D. 1987, *Ap. J. Suppl.*, **65**, 405.
 Cahn, J.H. and Kaler, J.B. 1971, *Ap. J. Suppl.*, **22**, 319.
 Capriotti, E. 1973, *Ap. J.*, **179**, 495.
 Cudworth, K.M. 1974, *A.J.*, **79**, 1384.
 Daub, C.T. 1982, *Ap. J.*, **260**, 612.
 Gathier, R. 1987, *Astr. and Ap. Suppl.*, **71**, 245.
 Gathier, R., Pottasch, S.R. and Goss, W.M. 1986b, *Astr. and Ap.*, **157**, 191.
 Gathier, R., Pottasch, S.R., Goss, W.M., and van Gorkom, J.H. 1983, *Astr. and Ap.*, **128**, 325.
 Gathier, R., Pottasch, S.R., and Pel, J.W. 1986a, *Astr. and Ap.*, **157**, 171.
 Hawley, S.A. 1978, *Pub. A.S.P.*, **90**, 370.
 Huggins, P.J. and Healy, A.P. 1986a, *Ap. J.*, **305**, L29.
 Huggins, P.J. and Healy, A.P. 1986b, *M.N.R.A.S.*, **220**, 33p.
 Kahn, F. 1983, in *IAU Symposium No. 103, Planetary Nebulae*, ed. R.D. Flower (Dordrecht: D. Reidel), p. 305.
 Kaler, J.B. 1970, *Ap. J.*, **160**, 881.
 Kaler, J.B. 1985, *Ap. J.*, **290**, 531.
 Kaler, J.B. 1986, *Ap. J.*, **308**, 322.
 Lenzuni, P., Natta, A., and Panagia, N. 1987, in *Planetary and Proto-Planetary Nebulae: from IRAS to ISO*, ed. A. Preite Martinez (Dordrecht: D. Reidel), p. 249.
 Mallik, D.C.V. and Peimbert, M. 1988, *Bull. A.A.S.*, **20**, 640.
 Masson, C.R. 1986, *Ap. J.*, **302**, L27.
 Méndez, R.H., Kudritzki, R.P., Herrero, A., Husfeld, D., and Groth, H.G. 1988, *Astr. and Ap.*, **190**, 113.
 Meyer, J.P. 1985, *Ap. J. Suppl.*, **57**, 151.
 Natta, A. and Panagia, N. 1981, *Ap. J.*, **248**, 189.
 O'Dell, C.R. 1962, *Ap. J.*, **135**, 371.
 Osterbrock, D.E. and Flather, E. 1959, *Ap. J.*, **129**, 26.
 Peimbert, M. 1985, *Rev. Mexicana Astron. Astrof.*, **10**, 125.
 Peimbert, M. and Torres-Peimbert, S. 1987a, *Rev. Mexicana Astron. Astrof.*, **14**, 540.
 Peimbert, M. and Torres-Peimbert, S. 1987b, *Rev. Mexicana Astron. Astrof.*, **15**, 117.
 Phillips, P. 1988, in *IAU Symposium No. 131, Planetary Nebulae*, ed. S. Torres-Peimbert (Dordrecht: Kluwer), in press.
 Phillips, J.P. and Pottasch, S.R. 1984, *Astr. and Ap.*, **130**, 91.
 Pottasch, S.R. 1980, *Astr. and Ap.*, **89**, 336.
 Pottasch, S.R. 1984, *Planetary Nebulae*, (Dordrecht: D. Reidel), p. 102.
 Pottasch, S.R. 1987, in *Late Stages of Stellar Evolution*, eds. S. Kwok and S.R. Pottasch (Dordrecht: D. Reidel), p. 355.
 Pottasch, S.R. et al. 1984, *Astr. and Ap.*, **138**, 10.
 Pwa, R., Pottasch, S.R., and Mo, J.E. 1986, *Astr. and Ap.*, **164**, 184.
 Rodríguez, L.F. 1988, in *IAU Symposium No. 131, Planetary Nebulae*, ed. S. Torres-Peimbert (Dordrecht: Kluwer), in press.
 Sabbadin, F., Gratton, R.G., Bianchini, A., and Ortolani, S. 1984, *Astr. and Ap.*, **136**, 181.
 Savage, B.D. and Mathis, J.S. 1979, *Ann. Rev. Astr. and Ap.*, **17**, 73.
 Schneider, S.E. and Terzian, Y. 1983, *Ap. J.*, **274**, L61.
 Seaton, M.J. 1966, *M.N.R.A.S.*, **132**, 113.
 Seaton, M.J. 1968, *Ap. Letters*, **2**, 55.
 Seaton, M.J. and Osterbrock, D.E. 1957, *Ap. J.*, **125**, 66.
 Shields, G.A. 1978, *Ap. J.*, **219**, 565.
 Shields, G.A. 1983, in *IAU Symposium No. 103, Planetary Nebulae*, ed. R.D. Flower (Dordrecht: D. Reidel), p. 259.
 Storey, J.W.V. 1984, *M.N.R.A.S.*, **206**, 521.
 Terzian, Y. and Dickey, J. 1973, *A.J.*, **78**, 875.
 Tifft, W.G., Connolly, L.P., and Webb, D.F. 1972, *M.N.R.A.S.*, **158**, 47.
 Torres-Peimbert, S. and Peimbert, M. 1977, *Rev. Mexicana Astron. Astrof.*, **2**, 181. TPP.
 Torres-Peimbert, S., Peimbert, M., and Peña, M. 1988, in preparation.
 Webster, B.L. 1969, *M.N.R.A.S.*, **143**, 79.
 Westerlund, B.E. and Henize, K.G. 1967, *Ap. J. Suppl.*, **14**, 154.
 Zuckerman, B. and Gatley, I. 1988, *Ap. J.*, **324**, 501.

D.C.V. Mallik: Indian Institute of Astrophysics, Bangalore 560034, India.

Manuel Peimbert: Instituto de Astronomía, UNAM, Apartado Postal 70-264, 04510 México, D.F., México.

